Mathematical Modeling and Stability Analysis of a Hybrid Five-Level Static VAR Compensation for Efficient Power Transmission

C.O. Omeje
Lecturer in the Department of Electrical/Electronic Engineering, University of Port Harcourt, Rivers State Nigeria.

Abstract

This paper presents a comprehensive analysis of a hybrid fault tolerant five-level voltage source inverter which is applied in the control of reactive power flow for a given transmission line. The mathematical modeling of this five-level Static Var Compensator formed by a cascade between a three-level flying capacitor and H-bridge in their d-q axis is presented in this work. A stability test analysis on the five-level based Static Var Compensator is illustrated herein. The stability test results gave determinant values of $-5.6674e^{-12}$ *and* $1.1335e^{-13}$ *for the controllability and observability matrixwith Eigen values of*$\lambda_1 = -2.01 + j314.16$, $\lambda_2 = -2.01 - j314.16$ *and* $\lambda_3 = -0.00$ *for marginal stability test condition. Furthermore, the application of this multi-level converter on high voltage direct current transmission (HVDC) with a back-to-back (B2B) converter produced a real power value of 2800KW which compensated for the reactive power value of -1800 KVARthat was generated along the transmission line. This compensation in real and reactive power ensured an almost unity power factor operation as presented in the simulation results. All simulation processes including open loop and closed loop were done in MATLAB 7.12.*

Key words: *Thyristor controlled Reactor, Hybrid Five-Level VSI, Static Var Compensator, State- Space Stability Test, Eigen Values, HVDC and Reactive power.*

Nomenclatures

SVC: Static Var Compensator
FACTS: Flexible Alternating Current Transmission System
HVDC: High Voltage Direct Current
TCR: Thyristor-Controlled Reactor
TCSC: Thyristor Controlled Series Compensator
IGBT: Insulated Gate Bipolar Transistors
THD: Total harmonic distortion
VSC: Voltage Source Converter
A.C: Alternating Current
VAR: Volts Ampere Reactive
α: Controlled delay angle
λ : Eigen Constant
m : Modulation Index

I. INTRODUCTION

Reactive power compensations and its control have formed an essential part in the analysis of power system and efficient functioning of transmission line parameters. This ideology is achieved through the minimization of power transmission losses by maintaining a constant supply voltage across the power line at near unity power factor [1]. It is a well-established fact that by using reactive power compensatory-device such as FACTS to control the magnitude of the voltage at a particular bus bar in any electric power system, the minimization of these transmission losses is actualized. Other FACTS-Compensatory Devices include Unified Power Flow Controller UPFC, Thyristor Controlled Reactor (TCR), Thyristor Controlled Series Compensator (TCSC) and Sub-Synchronous Resonance [2]-[5].

A Static Var Compensator (SVC) is an electrical device meant for providing fast-acting reactive power compensation on high-voltage electricity transmission network [6].SVC regulates the magnitude of the supply voltage and stabilizes the transmission network during transient disturbances [6].The SVC is an automated (mechanized) impedance matching device, designed to ensure that the transmission line parameters get closer to unity power factor. This can be realized through the following underlying principles: If the power systems reactive load is capacitive (leading Power factor), the SVC device switches on the reactors to absorb the reactive power from the system thus lowering the system voltage to the expected default value [7].

For an inductive load condition (Lagging Power factor), the capacitor banks are automatically switched on with the aid of a thyristor-controlled VSI.This process provides a higher but appreciable voltage magnitude [7].

II. PRINCIPLES OF OPERATION OF THE NOVEL FIVE-LEVEL VSI BASED STATIC COMPENSATOR

The Static Var Compensator that uses a five-level VSI as depicted in figure 1 consists of twenty-four

power IGBT switches that are connected to a three-phase supply through a reactor. The hybrid five-level topology was used in preference to the existing conventional three-level due to the following points [8]-[10]:

I. Enhancement of voltage quality of the proposed topology.

II. Obvious reduction in magnitude of percentage harmonics sequel to the increase in voltage level.

III. Improved power quality that is proportionate to increase in voltage level.

IV. Attenuation of electromagnetic interference from a reduced $\frac{dV}{dt}, \frac{di}{dt}$ stress and noise frequency.

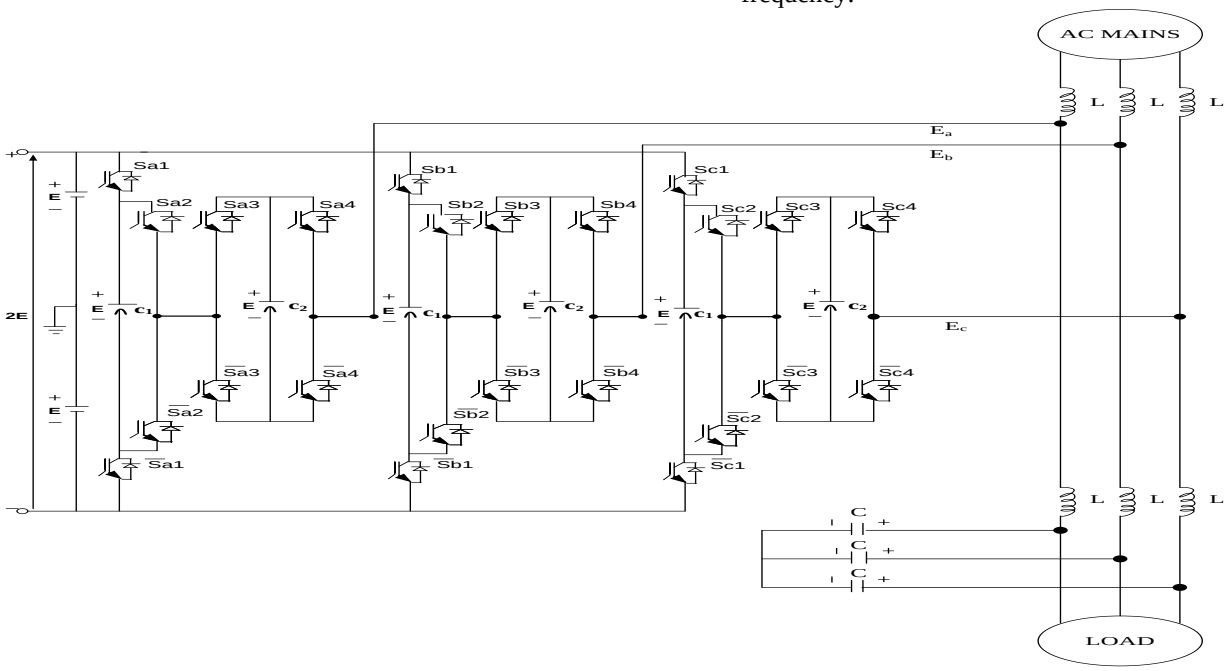

Figure.1 Power circuit of Five-level VSI Static Var Compensator

The power circuit of the proposed SVC topology is shown in figure 1. It employs a pulse-width modulated voltage source inverter that is connected to the a.c mains via a reactor **L**. A d.c capacitor is connected to the d.c terminal of the SVC. The capacitor ensures a ripple (Harmonic) free d.c voltage at the inverter input terminal and at the same time absorb excess reactive power [7]. The load terminal is connected to the inverter terminal through a second order filter comprising **L** and**C** that reduces the harmonic current components flowing into the grid.

The operational principle of the above SVC system can be explained by considering the per phase fundamental equivalent circuit as shown in figure 2a while figure 2b represents the phasor diagram for leading and lagging power factor characteristics. In the figure below, $\mathbf{E_{A1}}$ is the ac main voltage source. $\mathbf{I_{A1}}$ and $\mathbf{V_A}$ are the respective fundamental components of current and output voltage for the inverter supply. The SVC is connected to the ac mains through a reactor **L** and a resistor **R** representing the total loss in the circuit. As shown in figure 2b controlling the phase angle α of the inverter output voltage, the amplitude of the fundamental component $\mathbf{E_{A1}}$ can be controlled.

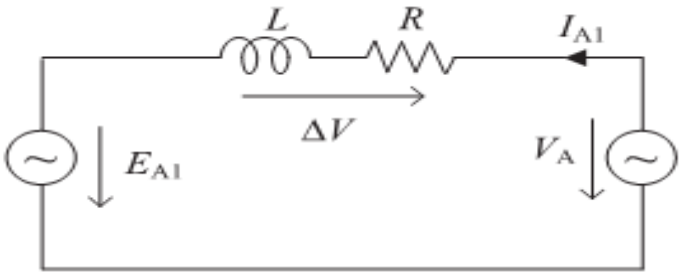

Figure 2a Per-Phase Fundamental Equivalent Circuit.

Figure 2b: Leading and Lagging power factor characteristic phasor diagram

III. CONTROL BLOCK AND MATHEMATICAL MODEL OF THE HYBRIDFIVE-LEVEL STATIC VAR COMPENSATOR

The control block diagram in figure 3 was applied in the generation of the firing signals of the five level voltage source inverter whereas figure 4 represents a simplified equivalent circuit of the 5-level voltage source inverter based Static Var Compensator.

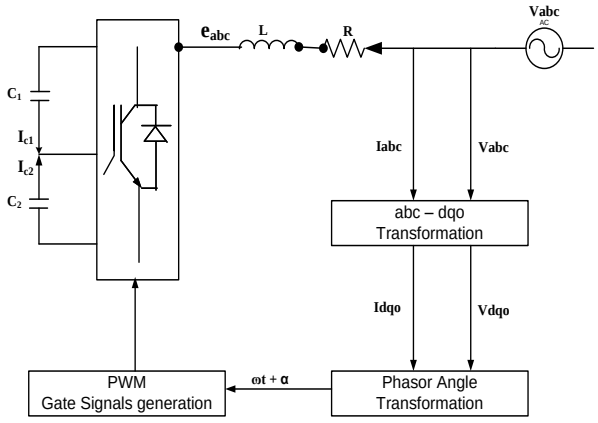

Figure 3: Control block diagram of the five-level VSI based Static Var Compensator.

The mathematical modeling of the circuit presented in figure 4 is effectively done by applying the Kirchhoff's voltage law (KVL) across the three phases of the inverter equivalent circuits.

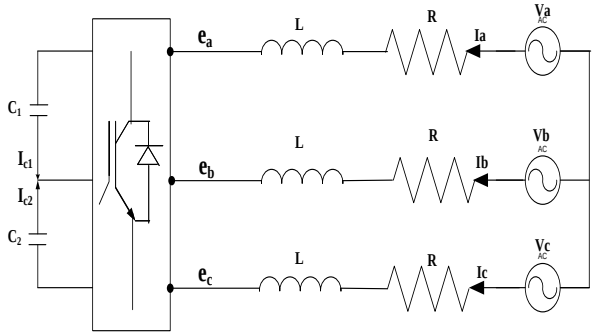

Figure 4 Three-Phase Equivalent Circuit of the Proposed SVC.

KVL in figure 4 gives rise to (1-3) as shown below:

$$\frac{di_a}{dt} = \frac{V_a - e_a}{L} - \frac{R}{L} i_a \quad (1)$$

$$\frac{di_b}{dt} = \frac{V_b - e_b}{L} - \frac{R}{L} i_b \quad (2)$$

$$\frac{di_c}{dt} = \frac{V_c - e_c}{L} - \frac{R}{L} i_c \quad (3)$$

Rearranging (1) -(3) in a compact form and inserting them into a matrix gives rise to (4).

$$\frac{d}{dt}\begin{bmatrix} i_a \\ i_b \\ i_c \end{bmatrix} = \begin{bmatrix} \frac{-R}{L} & 0 & 0 \\ 0 & \frac{-R}{L} & 0 \\ 0 & 0 & \frac{-R}{L} \end{bmatrix} \begin{bmatrix} i_a \\ i_b \\ i_c \end{bmatrix} + \frac{1}{L}\begin{bmatrix} V_a - e_a \\ V_b - e_b \\ V_c - e_c \end{bmatrix} \quad (4)$$

The d.c capacitor voltages are given by (5a) and (5b)

$$C\frac{dU_c}{dt} = I_c \quad (5a)$$

$$\frac{d}{dt}\begin{bmatrix} U_{c1} \\ U_{c2} \end{bmatrix} = \frac{1}{C}\begin{bmatrix} I_{c1} \\ I_{c2} \end{bmatrix} \quad (5b)$$

The three-phase AC-mains voltage is given by (6).Where V_L is the r.m.s line voltage.

$$V_{ABC} = \begin{bmatrix} V_A \\ V_B \\ V_c \end{bmatrix} = \sqrt{\frac{2}{3}} \times V_L \times \begin{bmatrix} \sin(\omega t) \\ \sin\left(\omega t - \frac{2\pi}{3}\right) \\ \sin\left(\omega t + \frac{2\pi}{3}\right) \end{bmatrix} \quad (6)$$

The inverter output voltage is given by (7).

$$E_{ABC} = \begin{bmatrix} e_a \\ e_b \\ e_c \end{bmatrix} = \sqrt{\frac{2}{3}} \times m \times U_c \times \begin{bmatrix} \sin(\omega t + \alpha) \\ \sin\left(\omega t - \frac{2\pi}{3} + \alpha\right) \\ \sin\left(\omega t + \frac{2\pi}{3} + \alpha\right) \end{bmatrix} \quad (7)$$

Where m represents the modulation index and α represents the thyristor controlled delay angle or the firing angle of the inverter switches.To transform the above equations into their d-q axes, the following conditions were considered [11]-[12]:

I. All the switches were considered ideal to reduce the forward (barrier) voltage.
II. The source voltages and source currents were balanced.
III. The total loses in the inverter were represented by the lumped resistor R.
IV. The total harmonic contents caused by the switching action were considered to be negligible.
V. The improved Park's transformation matrix was applied.

Since the source currents and voltages arebalanced. $U_{c1} = U_{c2} = U_c$ and $I_{c1} = I_{c2} = I_c$.
The improved Park's transformation matrix is given by (8).
p

$$= \sqrt{\frac{2}{3}}\begin{bmatrix} \cos(\omega t+\alpha) & \cos\left(\omega t-\frac{2\pi}{3}+\alpha\right) & \cos\left(\omega t+\frac{2\pi}{3}+\alpha\right) \\ \sin(\omega t+\alpha) & \sin\left(\omega t-\frac{2\pi}{3}+\alpha\right) & \sin\left(\omega t+\frac{2\pi}{3}+\alpha\right) \\ \frac{1}{\sqrt{2}} & \frac{1}{\sqrt{2}} & \frac{1}{\sqrt{2}} \end{bmatrix}$$

(8)
Therefore, transforming the **abc** ac mains voltage into**dq** axes voltage reference frame gives (9).

$$V_{qdo} = p\,V_{ABC} = \sqrt{\frac{2}{3}} \times A \times \sqrt{\frac{2}{3}} \times V_L \times B \quad (9)$$

Where A =

$$\begin{bmatrix} \cos(\omega t+\alpha) & \cos\left(\omega t-\frac{2\pi}{3}+\alpha\right) & \cos\left(\omega t+\frac{2\pi}{3}+\alpha\right) \\ \sin(\omega t+\alpha) & \sin\left(\omega t-\frac{2\pi}{3}+\alpha\right) & \sin\left(\omega t+\frac{2\pi}{3}+\alpha\right) \\ \frac{1}{\sqrt{2}} & \frac{1}{\sqrt{2}} & \frac{1}{\sqrt{2}} \end{bmatrix}$$

$B = \begin{bmatrix} \sin(\omega t) \\ \sin\left(\omega t-\frac{2\pi}{3}\right) \\ \sin\left(\omega t+\frac{2\pi}{3}\right) \end{bmatrix}$. Simplifying (9) gives (10)

$$V^1_{qdo} = \begin{bmatrix} V_q \\ V_d \\ V_o \end{bmatrix} = p\,V_{ABC} = \begin{bmatrix} -V_L \sin\alpha \\ V_L \cos\alpha \\ 0 \end{bmatrix} \quad (10)$$

The inverter output voltage in qdo axes is represented by (11)

$$E_{qdo} = p\,E_{ABC} = \sqrt{\frac{2}{3}} \times A \times \sqrt{\frac{2}{3}} \times m \times U_c \times Z \quad (11)$$

Where $Z = \begin{bmatrix} \sin(\omega t+\alpha) \\ \sin\left(\omega t-\frac{2\pi}{3}+\alpha\right) \\ \sin\left(\omega t+\frac{2\pi}{3}+\alpha\right) \end{bmatrix}$

A further simplification of (11) by matrix multiplication (12)

$$E^1_{qdo} = \begin{bmatrix} E_q \\ E_d \\ E_o \end{bmatrix} = p\,E_{ABC} = \begin{bmatrix} 0 \\ m \\ 0 \end{bmatrix} \times U_c \quad (12)$$

Transforming (4) current equation into qdo gives rise to (13)

$$\frac{d}{dt}\begin{bmatrix} i_q \\ i_d \end{bmatrix} = \begin{bmatrix} \frac{-R}{L} & -\omega \\ \omega & \frac{-R}{L} \end{bmatrix} \times \begin{bmatrix} i_q \\ i_d \end{bmatrix} + \frac{1}{L}\begin{bmatrix} V_q - e_q \\ V_d - e_d \end{bmatrix} \quad (13)$$

Substituting (10) and (12) into (13) gives rise to (14).

$$\frac{d}{dt}\begin{bmatrix} i_q \\ i_d \end{bmatrix} = \begin{bmatrix} \frac{-R}{L} & -\omega \\ \omega & \frac{-R}{L} \end{bmatrix} \times \begin{bmatrix} i_q \\ i_d \end{bmatrix} + \frac{1}{L}\begin{bmatrix} -V_L \sin\alpha \\ V_L \cos\alpha - mU_c \end{bmatrix} \quad (14)$$

The dc current converted to qdo gives rise to (15)

$$I_{c1} + I_{c2} = 2I_c = \sqrt{\frac{2}{3}} \times m \times i^1_{abc} \times Z \quad (15)$$

From $i_{qdo} = p\,i_{abc}$ (16)

$$i_{abc} = p^{-1} i_{qdo} \quad (17)$$

Where p^{-1} is the inverse Park's transformation matrix given by (18)

$$p^{-1} = \begin{bmatrix} \cos(\omega t+\alpha) & \sin(\omega t+\alpha) & 1 \\ \cos\left(\omega t-\frac{2\pi}{3}+\alpha\right) & \sin\left(\omega t-\frac{2\pi}{3}+\alpha\right) & 1 \\ \cos\left(\omega t+\frac{2\pi}{3}\right) & \sin\left(\omega t+\frac{2\pi}{3}+\alpha\right) & 1 \end{bmatrix} \quad (18)$$

Substituting (17) and (18) into (15) gives rise to (19).

$$2I_c = \sqrt{\frac{2}{3}} \times m \times \begin{bmatrix} \cos(\omega t+\alpha) & \sin(\omega t+\alpha) & 1 \\ \cos\left(\omega t-\frac{2\pi}{3}+\alpha\right) & \sin\left(\omega t-\frac{2\pi}{3}+\alpha\right) & 1 \\ \cos\left(\omega t+\frac{2\pi}{3}\right) & \sin\left(\omega t+\frac{2\pi}{3}+\alpha\right) & 1 \end{bmatrix} \times i^1_{qdo} \times Z \quad (19)$$

Further simplification of the above trigonometric functions applying identity reduction gives rise to (20a) and (20b).

$$2I_c = [0 \quad m \quad 0]\begin{bmatrix} i_q \\ i_d \\ i_o \end{bmatrix} = m\,i_d \quad (20a)$$

$$I_c = [0 \quad m \quad 0]\begin{bmatrix} i_q \\ i_d \\ i_o \end{bmatrix} = m\,\frac{i_d}{2} \quad (20b)$$

The capacitor voltage and current are obtained from (21a) and (21b)

$$\frac{dU_c}{dt} = \frac{I_c}{c} \quad (21a)$$

$$I_c = c\frac{dU_c}{dt} \quad (21b)$$

Substituting (20b) into (21b) with capacitor voltage differential been made subject of the formula gives rise to (22)

$$\frac{dU_c}{dt} = m\,\frac{I_d}{2c} \quad (22)$$

Total reactive power delivered by the proposed SVC is given by (23).

$$Q_c = V_q i_d - V_d i_q \quad (23)$$

Substituting (10) into (23) gives rise to (24).

$$Q_c = -V_L \sin\alpha\, i_d - V_L \cos\alpha\, i_q \quad (24)$$

Combining (14) and (22) then re-arranging them in state space gives rise to current equation presented in (25).

$$\frac{d}{dt}\begin{bmatrix} i_q \\ i_d \\ U_c \end{bmatrix} = \begin{bmatrix} \frac{-R}{L} & -\omega & 0 \\ \omega & \frac{-R}{L} & \frac{-m}{L} \\ 0 & \frac{m}{2C} & 0 \end{bmatrix}\begin{bmatrix} i_q \\ i_d \\ U_c \end{bmatrix} + \frac{1}{L}\begin{bmatrix} -V_L \sin\alpha \\ V_L \cos\alpha \\ 0 \end{bmatrix} \quad (25)$$

During a quiescent operating condition, (25) changes to (26).

$$\frac{d}{dt}\begin{bmatrix} i_{qo} \\ i_{do} \\ U_{co} \end{bmatrix} = \begin{bmatrix} \frac{-R}{L} & -\omega & 0 \\ \omega & \frac{-R}{L} & \frac{-m}{L} \\ 0 & \frac{m}{2C} & 0 \end{bmatrix} \begin{bmatrix} i_{qo} \\ i_{do} \\ U_{co} \end{bmatrix} + \frac{1}{L}\begin{bmatrix} -V_L \sin \alpha o \\ V_L \cos \alpha o \\ 0 \end{bmatrix} \quad (26)$$

In (26) the trigonometric function introduces a system with non-linearity. To achieve an easier design of the control system, (26) must be linearized under the following assumptions [13]-[14]:

I. A small disturbance $\Delta_{\alpha o}$ is applied to the variable in (25).
II. The second-order terms such as $(\cos \alpha)^2$ or $(\cos\Delta \alpha)^2$ and $(\sin \alpha)^2$ or $(\sin \Delta\alpha)^2$ are dropped or neglected.
III. The quiescent operating angle αo is near or equal to zero.

Applying a small disturbance to the variables in (25) around the operating point yields (27) -(31).

$$i_q = i_{qo} + \Delta i_q \quad (27)$$
$$i_d = i_{do} + \Delta i_d \quad (28)$$
$$U_c = U_{co} + \Delta U_d \quad (29)$$
$$\alpha = \alpha_o + \Delta\alpha \quad (30)$$
$$Q_c = Q_{co} + \Delta Q_c \quad (31)$$

Substituting (27), (28), (29), (30) and (31) into (25) gives rise to (32a) and (33b).

$$\frac{d}{dt}\begin{bmatrix} i_{qo} + \Delta i_q \\ i_{do} + \Delta i_d \\ U_{co} + \Delta U_c \end{bmatrix} = \begin{bmatrix} \frac{-R}{L} & -\omega & 0 \\ \omega & \frac{-R}{L} & \frac{-m}{L} \\ 0 & \frac{m}{2C} & 0 \end{bmatrix} \begin{bmatrix} i_{qo} + \Delta i_q \\ i_{do} + \Delta i_d \\ U_{co} + \Delta U_c \end{bmatrix} + \frac{1}{L}\begin{bmatrix} -V_L \sin(\alpha_o + \Delta\alpha) \\ V_L \cos(\alpha_o + \Delta\alpha) \\ 0 \end{bmatrix} \quad (32a)$$

$$\frac{d}{dt}\begin{bmatrix} i_{qo} \\ i_{do} \\ U_{co} \end{bmatrix} + \frac{d}{dt}\begin{bmatrix} \Delta i_q \\ \Delta i_d \\ \Delta U_c \end{bmatrix} = \begin{bmatrix} \frac{-R}{L} & -\omega & 0 \\ \omega & \frac{-R}{L} & \frac{-m}{L} \\ 0 & \frac{m}{2C} & 0 \end{bmatrix} \begin{bmatrix} i_{qo} \\ i_{do} \\ U_{co} \end{bmatrix} +$$

$$\begin{bmatrix} \frac{-R}{L} & -\omega & 0 \\ \omega & \frac{-R}{L} & \frac{-m}{L} \\ 0 & \frac{m}{2C} & 0 \end{bmatrix} \begin{bmatrix} \Delta i_q \\ \Delta i_d \\ \Delta U_c \end{bmatrix} + \frac{1}{L}\begin{bmatrix} -V_L \sin(\alpha_o + \Delta\alpha) \\ V_L \cos(\alpha_o + \Delta\alpha) \\ 0 \end{bmatrix} \quad (32b)$$

Subtracting (26) from (32b) yields (33).

$$\frac{d}{dt}\begin{bmatrix} \Delta i_q \\ \Delta i_d \\ \Delta U_c \end{bmatrix} = \begin{bmatrix} \frac{-R}{L} & -\omega & 0 \\ \omega & \frac{-R}{L} & \frac{-m}{L} \\ 0 & \frac{m}{2C} & 0 \end{bmatrix} \times \begin{bmatrix} \Delta i_q \\ \Delta i_d \\ \Delta U_c \end{bmatrix} +$$

$$\frac{1}{L}\begin{bmatrix} (V_L \sin \alpha_o - V_L \sin(\alpha_o + \Delta\alpha)) \\ (-V_L \cos \alpha_o + V_L \cos(\alpha_o + \Delta\alpha)) \\ 0 \end{bmatrix} \quad (33)$$

Rearranging (33) gives rise to (34)

$$\frac{d}{dt}\begin{bmatrix} \Delta i_q \\ \Delta i_d \\ \Delta U_c \end{bmatrix} = \begin{bmatrix} \frac{-R}{L} & -\omega & 0 \\ \omega & \frac{-R}{L} & \frac{-m}{L} \\ 0 & \frac{m}{2C} & 0 \end{bmatrix} \begin{bmatrix} \Delta i_q \\ \Delta i_d \\ \Delta U_c \end{bmatrix} +$$

$$\frac{1}{L}\begin{bmatrix} V_L(\sin \alpha_o - \sin(\alpha_o + \Delta\alpha)) \\ V_L(\cos(\alpha_o + \Delta\alpha) - \cos \alpha_o) \\ 0 \end{bmatrix} \quad (34)$$

Analyzing the above trigonometric functions using the conventional rules in [15] and in (35) and (36) give rise to (37) and (38):

$$\sin A - \sin B = 2\cos\left(\frac{A+B}{2}\right)\sin\left(\frac{A-B}{2}\right) \quad (35)$$

$$\cos A - \cos B = 2\sin\left(\frac{A+B}{2}\right)\sin\left(\frac{A-B}{2}\right) \quad (36)$$

$$\sin \alpha_o - \sin(\alpha_o + \Delta\alpha) = 2\cos\left(\frac{2\alpha_o + \Delta\alpha}{2}\right)\sin\left(\frac{-\Delta\alpha}{2}\right) \quad (37)$$

$$\cos(\alpha_o + \Delta\alpha) - \cos \alpha_o = 2\sin\left(\frac{\alpha_o + \Delta\alpha + \alpha_o}{2}\right)\sin\left(\frac{\alpha_o + \Delta\alpha - \alpha_o}{2}\right) \quad (38)$$

Applying the third assumption that is $\alpha_o \to 0$ in (37) gives rise to (39)

$$2\cos\left(\frac{\Delta\alpha}{2}\right)\sin\left(\frac{-\Delta\alpha}{2}\right) = -2\cos\left(\frac{\Delta\alpha}{2}\right)\sin\left(\frac{\Delta\alpha}{2}\right)$$
$$= -\sin\left(\frac{\Delta\alpha}{2} + \frac{\Delta\alpha}{2}\right) = -\sin(\Delta\alpha)$$
$$= \sin(-\Delta\alpha) \quad (39)$$

Applying the first assumption that is Δα being very smallsuch

that $-\sin(\Delta\alpha) = \sin(-\Delta\alpha) \cong \Delta\alpha$ (40)

Also applying the third assumption that is $\alpha_o \to 0$ in (38) gives rise to (41)

$$2\sin\left(\frac{2\alpha_o + \Delta\alpha}{2}\right)\sin\left(\frac{\Delta\alpha}{2}\right) = 2\sin\left(\frac{\Delta\alpha}{2}\right)\sin\left(\frac{\Delta\alpha}{2}\right)$$
$$= 2\left(\sin\frac{\Delta\alpha}{2}\right)^2 \quad (41)$$

Also the second assumption gives (42) that is dropping all second order term such that

$$2\left(\sin\frac{\Delta\alpha}{2}\right)^2 \to 0 \quad (42)$$

Substituting the values of the above-reduced trigonometry gives a linearized equation represented by (43)

$$\frac{d}{dt}\begin{bmatrix} \Delta i_q \\ \Delta i_d \\ \Delta U_c \end{bmatrix} = \begin{bmatrix} \frac{-R}{L} & -\omega & 0 \\ \omega & \frac{-R}{L} & \frac{-m}{L} \\ 0 & \frac{m}{2C} & 0 \end{bmatrix} \begin{bmatrix} \Delta i_q \\ \Delta i_d \\ \Delta U_c \end{bmatrix} + \frac{1}{L}\begin{bmatrix} V_L \\ 0 \\ 0 \end{bmatrix} \Delta\alpha \quad (43)$$

At a quiescent operating point, the reactive power delivered by the proposed SVC is given by (44).

$$Q_{co} = -V_L \sin\alpha_o\, i_{do} - V_L \cos\alpha_o\, i_{qo} \quad (44)$$

During a slight disturbance, (27), (28), (29), (30) and (31) are substituted into (44) to giving rise to (45).

$$Q_{co} + \Delta Q_c = -V_L \sin(\alpha_o + \Delta\alpha)\, i_{do} - V_L \sin(\alpha_o + \Delta\alpha)\, \Delta i_d - V_L \cos(\alpha_o + \Delta\alpha)\, i_{qo} - V_L \cos(\alpha_o + \Delta\alpha)\, \Delta i_q \quad (45)$$

Therefore, subtracting (44) from (45) results to (46)

$$\Delta Q_c = -V_L \sin(\alpha_o + \Delta\alpha)\, i_{do} + V_L \sin\alpha_o\, i_{do} - V_L \cos(\alpha_o + \Delta\alpha)\, i_{qo} + V_L \cos\alpha_o\, i_{qo} - V_L \sin(\alpha_o + \Delta\alpha)\, \Delta i_d - V_L \cos(\alpha_o + \Delta\alpha)\, \Delta i_q \quad (46)$$

Rearranging (46) results to (47)

$$\Delta Q_c = -V_L(\sin(\alpha_o + \Delta\alpha) - \sin\alpha_o) i_{do} - V_L(\cos(\alpha_o + \Delta\alpha) - \cos\alpha_o) i_{qo} - V_L \sin(\alpha_o + \Delta\alpha)\, \Delta i_d - V_L \cos(\alpha_o + \Delta\alpha)\, \Delta i_q \quad (47)$$

Applying the trigonometric identity given in (35) and (36) results to (48)

$$\sin(\alpha_o + \Delta\alpha) - \sin\alpha_o = 2\cos\left(\frac{2\alpha_o + \Delta\alpha}{2}\right)\sin\left(\frac{\Delta\alpha}{2}\right) \quad (48)$$

Applying the third assumption that is $\alpha_o \to 0$, (48) transforms into (49).

$$2\cos\left(\frac{\Delta\alpha}{2}\right)\sin\left(\frac{\Delta\alpha}{2}\right) = \sin\left(\frac{\Delta\alpha}{2} + \frac{\Delta\alpha}{2}\right) = \sin(\Delta\alpha) \cong \Delta\alpha \text{ as } \Delta\alpha \ll 1 \quad (49)$$

Since

$$\cos(\alpha_o + \Delta\alpha) - \cos\alpha_o = 2\sin\left(\frac{2\alpha_o + \Delta\alpha}{2}\right)\sin\left(\frac{\Delta\alpha}{2}\right) 2\sin\left(\frac{\Delta\alpha}{2}\right)\sin\left(\frac{\Delta\alpha}{2}\right)$$

$$2\left(\sin\frac{\Delta\alpha}{2}\right)^2 \to 0$$

$$\sin(\alpha_o + \Delta\alpha) = \sin\alpha_o \cos\Delta\alpha + \sin\Delta\alpha\cos\alpha_o = \sin\Delta\alpha \cong \Delta\alpha \text{ as } \alpha_o \to 0$$

$$\cos(\alpha_o + \Delta\alpha) = \cos\alpha_o \cos\Delta\alpha + \sin\Delta\alpha\sin\alpha_o = \cos\Delta\alpha \cong 1 \text{ as } \alpha_o \to 0$$

and $\Delta\alpha \ll 1$

Substituting these reduced trigonometric functions into (47) produces (50).

$$\Delta Q_c = -V_L(\Delta\alpha) i_{do} - V_L(\Delta\alpha)\Delta i_d - V_L \Delta i_q \quad (50)$$

Since $\Delta\alpha \ll 1$, then $\Delta Q_c \cong -V_L \Delta i_q$ (51)

The overall state space equations are presented by (52a) and (52b).

$$\frac{d}{dt}\begin{bmatrix}\Delta i_q \\ \Delta i_d \\ \Delta U_c\end{bmatrix} = \begin{bmatrix}\frac{-R}{L} & -\omega & 0 \\ \omega & \frac{-R}{L} & \frac{-m}{L} \\ 0 & \frac{m}{2C} & 0\end{bmatrix}\begin{bmatrix}\Delta i_q \\ \Delta i_d \\ \Delta U_c\end{bmatrix} + \frac{1}{L}\begin{bmatrix}V_L \\ 0 \\ 0\end{bmatrix}\Delta\alpha \quad (52a)$$

$$\Delta Q_c = [-V_L \quad 0 \quad 0]\begin{bmatrix}\Delta i_q \\ \Delta i_d \\ \Delta U_c\end{bmatrix} \quad (52b)$$

The dynamic equations are derived as follows:

$$\dot{X}(t) = AX(t) + BU(t) \quad (53)$$

$$Y = CX(t) \quad (54)$$

Where: $\dot{X}(t) = \begin{bmatrix}\frac{di_q}{dt} \\ \frac{di_d}{dt} \\ \frac{dU_c}{dt}\end{bmatrix}$; $X(t) = \begin{bmatrix}i_q \\ i_d \\ U_c\end{bmatrix}$;

$$A = \begin{bmatrix}\frac{-R}{L} & -\omega & 0 \\ \omega & \frac{-R}{L} & \frac{-m}{L} \\ 0 & \frac{m}{2C} & 0\end{bmatrix}; \quad B = \begin{bmatrix}\frac{-V_L}{L} \\ 0 \\ 0\end{bmatrix};$$

$C = [-V_L \quad 0 \quad 0]$; $U(t) = \Delta\alpha$.

The Laplace transformation is derived as follows:

$$SX(s) - X(0) = AX(s) + BU(s) \quad (55a)$$

$$Y(s) = CX(s) \quad (55b)$$

Simplifying (55a) and (55b) with $X(0)$ set to zero produces (56)

$$SX(s) = AX(s) + BU(s) \quad (56)$$

$$X(s) = [SI - A]^{-1}BU(s) \quad (57)$$

Substituting (57) into (55b) gives rise to (58)

$$Y(s) = C[SI - A]^{-1}BU(s) \quad (58)$$

$$\frac{Y(s)}{U(s)} = \frac{\Delta Q_{c(s)}}{\Delta\alpha_{(s)}} = C[SI - A]^{-1}B \quad (59)$$

$$[SI - A]^{-1} = \frac{\text{Adjoint of } [SI - A]}{\text{Determinant of } [SI - A]} \quad (60)$$

Where Adjoint of $[SI - A] = C^T =$

$$\begin{bmatrix}s^2 + \frac{SR}{L} + \frac{m^2}{2LC} & -s\omega & \frac{m\omega}{L} \\ s\omega & s^2 + \frac{SR}{L} & \frac{-Sm}{L} - \frac{Rm}{L^2} \\ \frac{m\omega}{2C} & \frac{Sm}{2C} + \frac{Rm}{2LC} & s^2 + \frac{SR}{L} + \frac{m^2}{2LC}\end{bmatrix} \quad (61)$$

Determinant of $[SI - A] =$

$$s^3 + \frac{2R}{L}s^2 + \left[\left(\frac{R}{L}\right)^2 + \frac{m^2}{2LC} + \omega^2\right]s + \frac{m^2R}{2L^2C} \quad (62)$$

Substituting (61) and (62) into (60) produces the actual transfer function represented in (63).

$$\frac{\Delta Q_{c(s)}}{\Delta\alpha_{(s)}} = C[SI - A]^{-1}B = \frac{\frac{V_L^2}{L}\left[s^2 + \frac{R}{L}s + \frac{m^2}{2LC}\right]}{s^3 + \frac{2R}{L}s^2 + \left[\left(\frac{R}{L}\right)^2 + \frac{m^2}{2LC} + \omega^2\right]s + \frac{m^2R}{2L^2C}} \quad (63)$$

The parameters presented below were applied to the above transfer function to test for system stability.

R = 10Ω, V_L = 415v, L = 100 mH, F = 50Hz, m = 0.8, C = 1000μF. Direct substitution of these values gives (64)

$$\frac{\Delta Q_{c(s)}}{\Delta\alpha_{(s)}} = C[SI - A]^{-1}B = \frac{17222500(s^2 + 100s + 320000)}{s^3 + 200s^2 + 428696.04s + 32000000} \quad (64)$$

The stability test carried out on the proposed SVC gave the following results:

Controllability matrix

$$= 1 \times 10^{7} \begin{bmatrix} -0.0001 & 0.0002 & 8.2265 \\ 0 & -0.0262 & 0.1052 \\ 0 & 0 & -0.0026 \end{bmatrix}$$

Observability matrix

$$= 1 \times 10^{7} \begin{bmatrix} -0.0000 & 0 & 0 \\ 0.0001 & 0.0130 & 0.1052 \\ 0 & -0.0524 & -0.0209 \end{bmatrix}$$

Determinant of Controllability matrix $= -5.6674e^{12}$

Determinant of Observability matrix $= 1.1335e^{13}$

Eigen Values of the system transmittance matrix

$$= 1.0 \times 10^{2} \begin{bmatrix} -0.0201 + j3.1416 \\ -0.0201 - j3.1416 \\ -0.0000 \end{bmatrix}$$

The above computed results showed that the determinants of the system controllability and observability matrix are $-5.6674e^{12}$ and $1.1335e^{13}$ with a non-zero value. Thus, the system at this point is stable. In like manner, the Eigen values of the system transmittance matrix are $\lambda_1 = -2.01 + j314.16$, $\lambda_2 = -2.01 - j314.16$ and $\lambda_3 = -000$. These Eigen values confirm that the system is marginally stable due to the obvious variation in the positive and negative values of the complex conjugates of λ_1, λ_2 and λ_3 .The step response of the above Reactive Power in open loop transfer function is shown in figure 5.

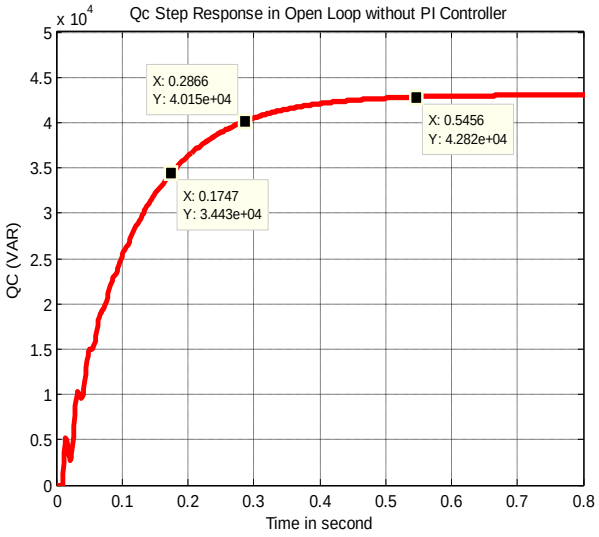

Figure 5Step Response of Equation (64) OpenLoop SVC Reactive Power Controlled System.

Introducing a PI-controller and a feed-back sensor, an improved dynamic response is achieved. The Simulink diagram representing a complete closed loop hybrid SVC model with a reactive power feedback sensor is given in figure 6 while the closed loop step response is represented in figure 7. A comparison between the two step responses in open and closed loop PI-controlled systems in terms of rise time, peak time, settling time and overall dynamic response was achieved in figure 8.

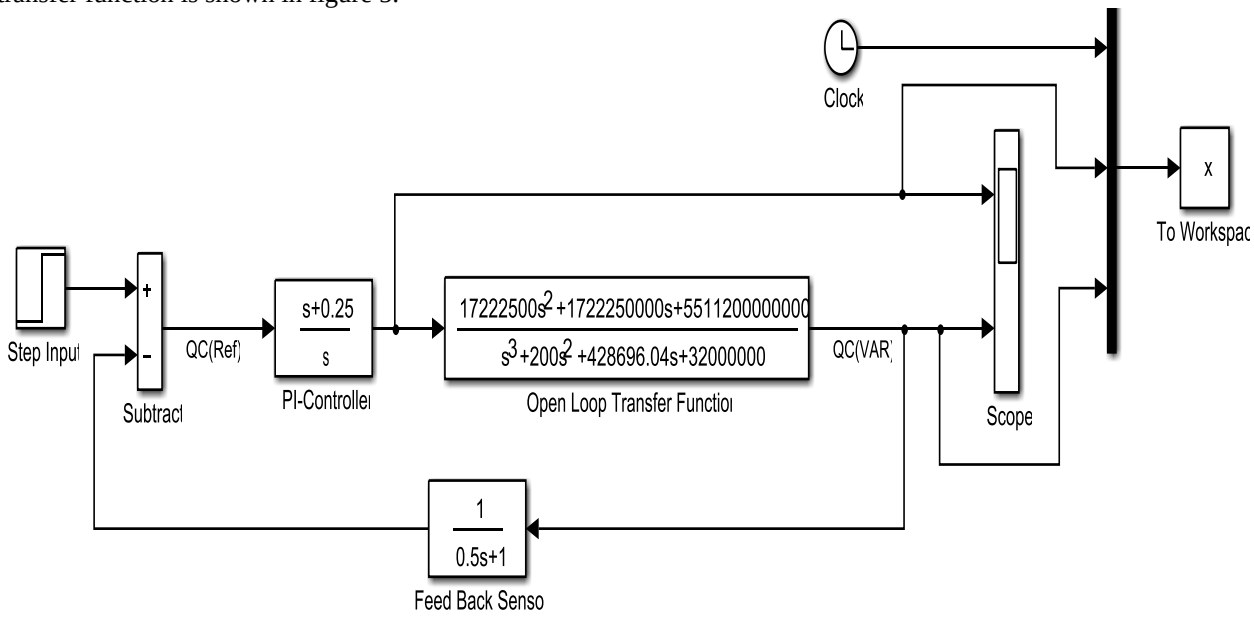

Figure 6 Simulink Model of the PI Controlled SVC Reactive Power.

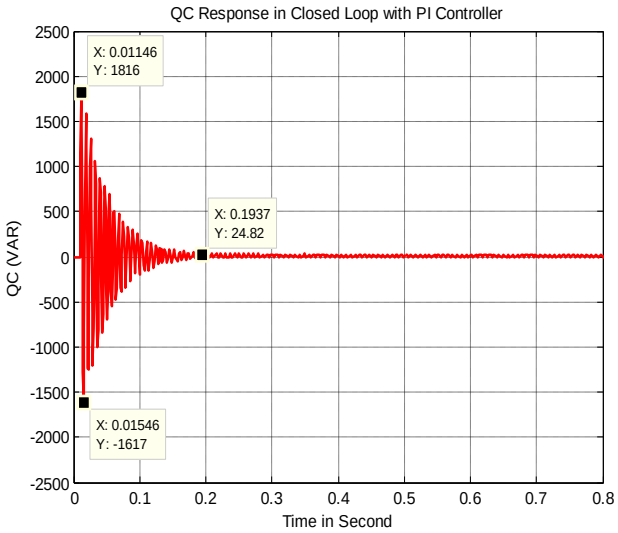

Figure 7 Step Response of the PI Controlled SVC Reactive Power.

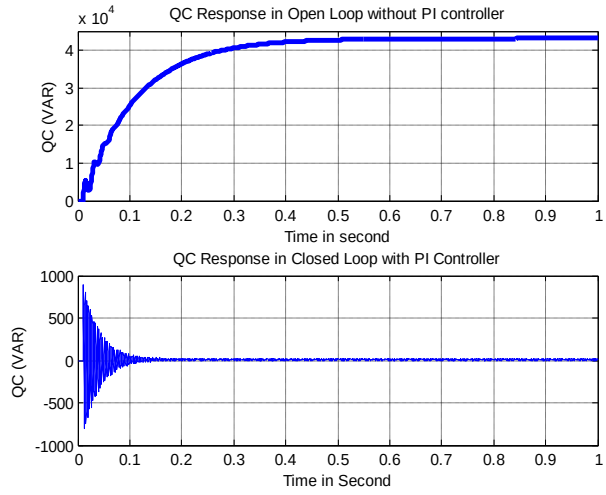

Figure 8 Step Responses of the Open loop and closed loop SVC controlled System.

From figures 5 and 7, the following characteristics were achieved: open loop step response rise time = 0.1747Second, Peak time = 0.2866Second, Settling time = 0.5456Second. Closed loop step response rise time = 0.01146Second, Peak time = 0.01546Second, Settling time = 0.1937Second. At steady state the magnitude of reactive power in open loop increased exponentially as 42,820VAR as against 24.82VAR achieved in closed loop as shown in figures 5 and 7.

IV. DYNAMIC RESPONSE OF THE HYBRID MULTI-LEVEL CONVERTER TO A HVDC (B2B) NETWORK

A back-to-back (B2B) converter is employed in the transmission of high voltage and power to the load centers at a synchronized frequency and voltage magnitude [17].Conventionally, electrical plants generate power in the form of **a.c** voltages and currents. This power is transmitted to the load centers on a three-phase base via **a.c** transmission lines. However, under certain circumstances, it is economically attractive to transmit a large amount of power over a long distance from remote areas using high voltage direct current (HVDC) method. This is because it is environmentally friendly and devoid of pollution. This breakeven in distance for HVDC overhead transmission lines usually lies in a range of 300-400 miles but smaller for underwater cables [18]. Although factors such as improved transient stability and dynamic damping of the electrical system oscillations influence the selection of the d.c transmission in preference to the **a.c** transmission. It is possible to interconnect two **a.c** systems that differ in their frequency values by means of a B2B converter in form of HVDC that ensures good frequency synchronization. Figure 13 represents a back-to-back (B2B) converter where HVDC is derived. This scheme consists of a three-phase full bridge converter that rectifies the a.c supply voltage to a d.c voltage. A large capacitor sandwiched between the rectifier and the inverter serves as a d.c-link to the proposed three phase five-level topology. This topology converts the d.c voltage to an a.c voltage with a synchronized frequency value that corresponds with the grid voltage [18]. LC filters are usually inserted at the inverter output terminal to remove the current harmonics generated by the converters from infiltrating into the grid. Furthermore, the power factor corrective capacitors are included with the **a.c** filter to correct the lagging reactive power also referred to as the inductive VARS. The control block diagram in figure 3 was used in the generation of the firing pulses presented in figure 9. The gating signals **ga3**, **ga4, ga7** and **ga8** are complementary to **ga1, ga2, ga5** and **ga6** respectively. The inverter output current and voltages are presented in figures 10-12.

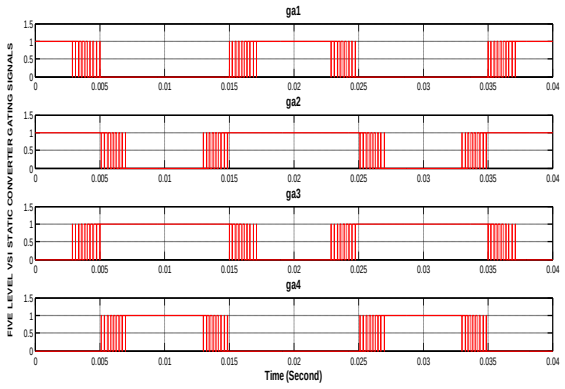

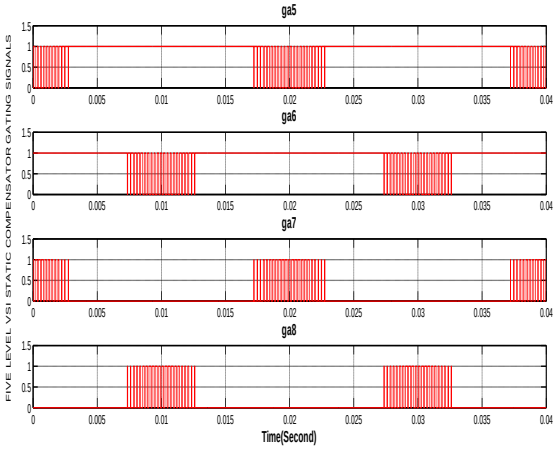

Figure 9: Five Level VSI Based Static Var Compensator Gating Signals

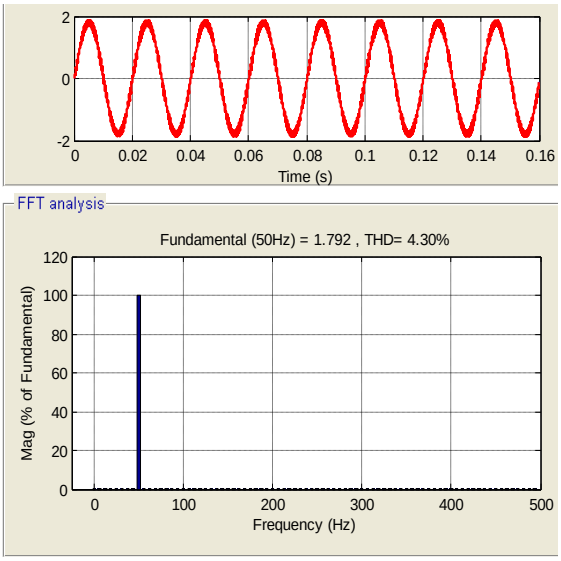

Figure 10: Phase Current of 5-level Inverter with Spectral Result. Fc = 4 KHz, MI = 0.8.

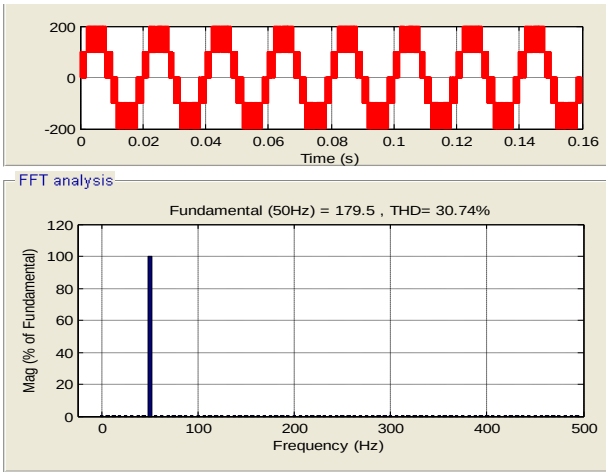

Figure 11: Phase Voltage of 5-level Inverter with Spectral Result. Fc = 4 KHz, MI = 0.8.

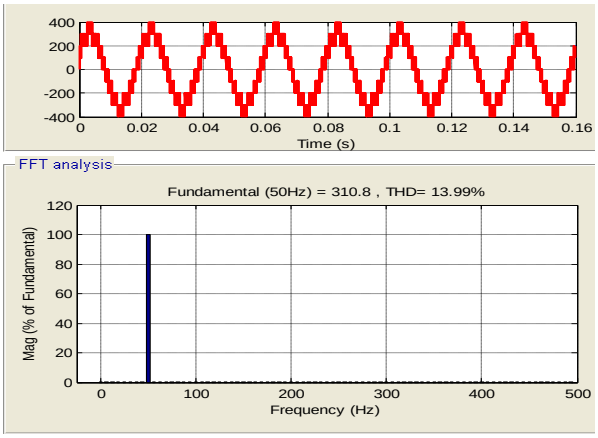

Figure 12: Line Voltage (VAB) of 5-level Inverter with Spectral Result. Fc = 4 KHz, MI = 0.8.

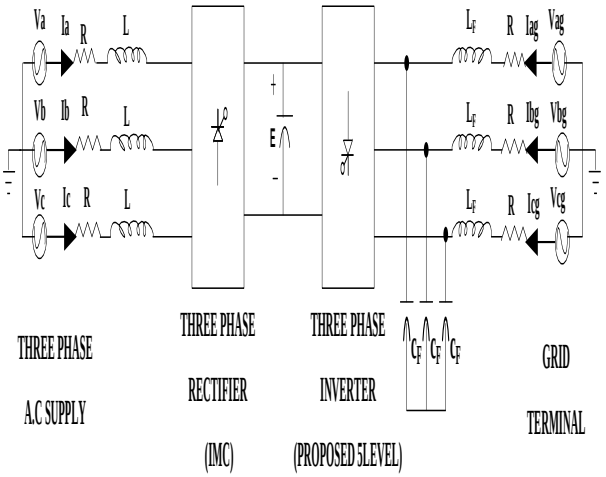

Figure 13: Back-to-Back (B2B) Converter System.

High Voltage Direct Current (HVDC) transmission using a B2B converter system that is made up of a rectifier and a five-level inverter was simulated to determine the real and reactive power variations on the grid. Analysis of the three phase grid currents and voltages showing their similarity in terms of power factor was also carried out. The results are presented in figures 11, 12a and 12b. The Simulink model is presented in figure 17. Converter 1 of the B2B operates as an uncontrollable rectifier through which a small quantity of real power flows from the **ac** to **dc** terminus while converter 2 operates as an inverter where the real power flows in the reverse direction [19]. At quiescent condition when converter 2 is not conducting, the capacitor C is charged to the peak value of the supply voltage through converter 1 and remains constant provided there is no real power transfer between the circuit and the supply. Conversely, when the switches of converter 2 conduct, real power is transferred from the **dc** terminal to the **ac**. In this way, the dc capacitor voltage is decreased and a reactive power is absorbed

by the SVC system (lagging mode). However, when the dc capacitor voltage is increased, a reactive power is generated by the SVC (leading mode) [20].

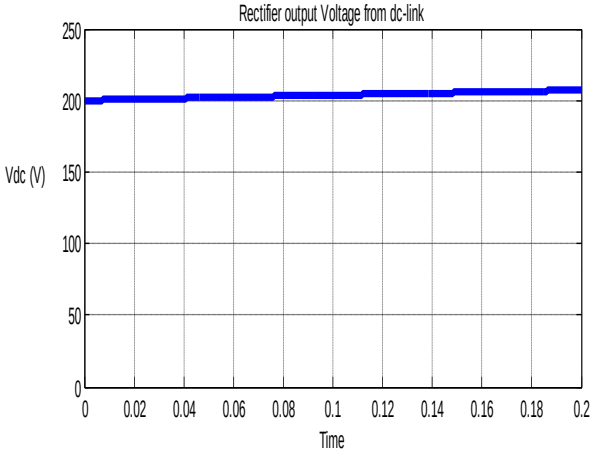

Figure 14: A Stiff D.C Voltage Supply.

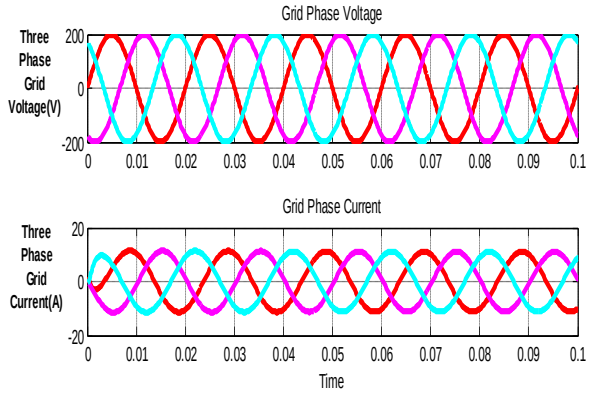

Figure 15a: Three Phase Grid Voltage and Current.

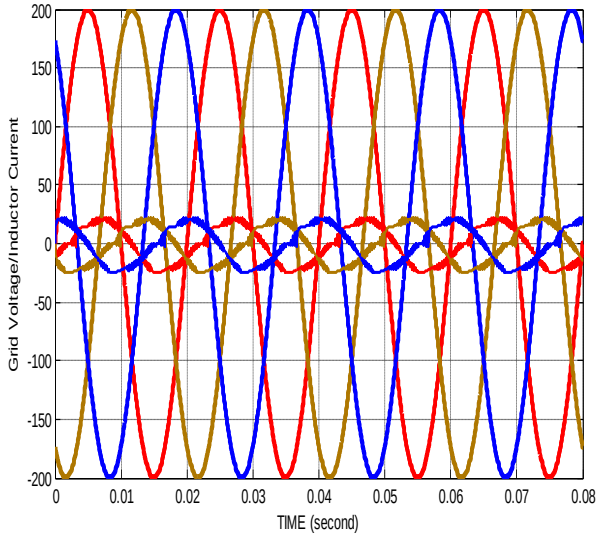

Figure 15b: An Interfaced Three Phase Grid Voltage and Current.

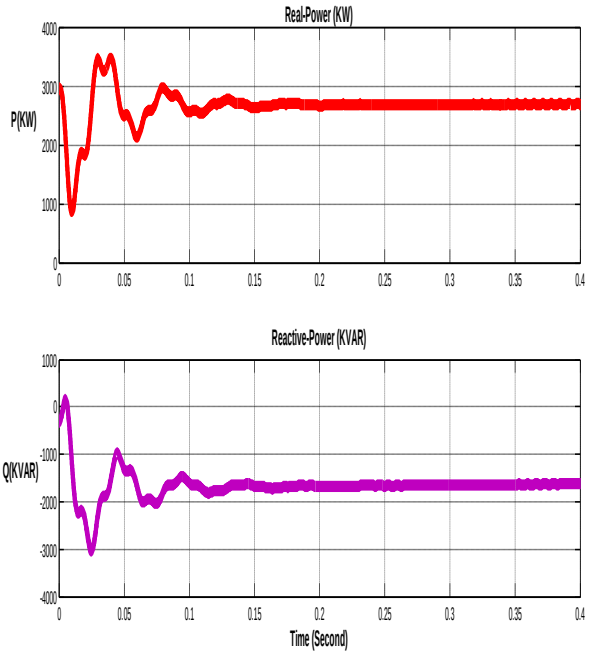

Figure 16: Real and Reactive Power Generated.

Figures 15a and 15b show the simulation results obtained for the grid-connected mode. Figure 15b indicates that grid current is almost in phase with the grid voltage with a slight phase lag. At steady state condition, a real power value of 2800KW at 0.175secondwas injected to compensate for the reactive power value of -1800KVAR so as to maintain almost a unity power factor on the grid as shown in figure 16.

V. CONCLUSIONS

This paper considered the equation modeling of a hybrid Five-level Static Var Compensator (SVC) and its stability test. The stability analysis performed using the controllability, observability and Eigen vector criteria deduced from the characteristic equation, proved that the system under analysis is marginally stable. This is confirmed from the Eigen values reported in subsection 3. The time response of the modeled topology at closed loop condition indicates that a good response performance is achieved with a PI-controller as proven in figures 5 and 7. In Figures 15a and 15b, the simulation results obtained for the grid-connected mode indicates that grid current is almost in phase with the grid voltage with a slight phase lag emanating from the 25μF shunt capacitor. The hybrid converter thus, injects a real power value to compensate for the more reactive loss thusensuring an almost a unity power factor value on the grid as shown in figure 16.

REFERENCES

[1] Xiao-Ping, Z. Rehtanz, C. Bikash, P. Flexible AC Transmission Systems: Modeling and Control. Springer publishers Berlin Heidelberg New York, 2006.

[2] Hingorani, N.G. Gyugyi L. Understanding FACTS: Concepts and Technology of flexible AC Transmission System, Institute of Electrical and Electronic Engineers, New York, 2000.

[3] Enrique Acha, Claudio Fuerte-Esquivel, Hugo Ambriz-Perez and Cesar Angeles-Camacho, "FACTS Modeling and Simulation in Power Networks".John Wiley and sons, New York, 2004.

[4] Kejun L., Jianguo Z., Chenghui Z. and Wei-Jen L. Dynamic simulator for thyristor-controlled series capacitor. IEEE Trans. Ind. Appli., Vol. 46 pp.1096-1102, 2010.

[5] Ambriz – Perez H. Acha, E. and Fuerte-Esquivel C.R. "Advanced SVC models For Newton-Raphson Load Flow and Newton Optimal Power flow studies". IEEE Trans Power Systems 15(1), pp.129-136, Nov. 2000.

[6] Fuerte-Esquivel, C.R. Acha, E. Ambriz-Perez, H. "Integrated SVC and step-down transformer model for Newton-Raphson load flow studies", IEEE Power Engineering Review 20(2), pp. 45-46, 2000.

[7] Kale M, Ödzemir E. Harmonic and reactive power compensation with shunt active power filter under non-ideal mains voltage. Electric Power Systems Research.Vol.74, N0.3, pp. 363-370, 2005.

[8] Bouzidi M, Bouafia S, Bouzidi A, Benaissa A, Barkat S. "Application of Backstepping to the Virtual Flux Direct Power Control of Five-Level Three-Phase Shunt Active Power Filter". International Journal of Power Electronics and DriveSystem (IJPEDS).Vol. 4, N0.2, pp.173–191, 2014.

[9] Saad S, Zellouma L. "Fuzzy Logic Controller for Three Level Shunt Active Filter Compensating Harmonics and Reactive Power". Electric Power Systems Research.Vol.79, N0.10, pp.1337-1341, 2009.

[10] Xiong, L. Poh Chiang,L. Peng, W. Blaabjerg,F. Tang,Yi. and Essam A. Al-Ammar, "Distributed Generation Using Matrix converter In Reverse Power Mode". IEEE Transactions on Power Electronics Vol. 28, No.3, March, 2013.

[11] BENGHANEM, M.—DRAOU, A. "A New Modeling and Control Analysis of an Advanced Static Var Compensator using a Three Level (Npc) Inverter Topology, J. Electrical Engineering

[12] Vol. 57 No. 5 (2006), pp. 285-290, 2006.

[13] Banga, A. and Kaushik, S.S. Modeling and simulation of SVC controller for enhancement of power system stability, International Journal of Advances in Engineering & Technology, Vol. 3, issue 9, pp. 79-84, 2011.

[14] Azeddine, Draou "An Advanced Static Var Compensator Based on A Three Level IGBT Inverter Modeling Analysis and Active Power Filtering". Journal of Electrical Engineering, Vol.63, No.6, pp. 392-396, 2012.

[15] Benghanem, M. and Draou, A. "A New Modeling and Control Analysis of An advanced Static Var Compensator Using A Three-Level (NPC) Inverter Topology, Journal of Electrical Engineering, Vol. 57, N0.5 2006, pp.285-290.

[16] Dass, H.K. Advanced Engineering Mathematics, S.Chand and Company ltd, NewDelhi.2010.

[17] Sindhu MR, Nair G, Manjula, Nambiar TNP. "Dynamic Power Quality Compensator with an Adaptive ShuntHybrid Filter".International Journal of Power Electronics and Drive System (IJPEDS).Vol.4, No. 4, pp.508–516, 2014.

[18] EdrisPouresmaeil, Daniel Montesinos-Miracle, Oriol Gomis-Bellmunt, Antoni Sudrià-Andreu. "Instantaneous Active and Reactive Current Control Technique of Shunt Active Power Filter Based On The Three-Level NPC Inverter". European Transactions on Electrical Power System.Vol. 21 No.7, pp. 2007–2022, 2011.

[19] ChaghiAbdelaziz, Guetta Amor, BenoudjitAzzedine. Four–legged active power filter compensation for a utility distribution system. Journal of Electrical Engineering.Vol. 55 N0.2, pp.31-35, 2004.

[20] Oltean, S.E. "Modern Control Of Static Var Compensator For Power System Stability enhancement, Scientific Bulletin of the PetruMaior" University of TîrguMureş, Vol. 9 No.1, pp. 33-37, 2012.

[21] Banga, A. and Kaushik, S.S. "Modeling and simulation of SVC controller for enhancement of power system stability". International Journal of Advances in Engineering & Technology, Vol. 3, issue 9, pp.79-84, 2011.

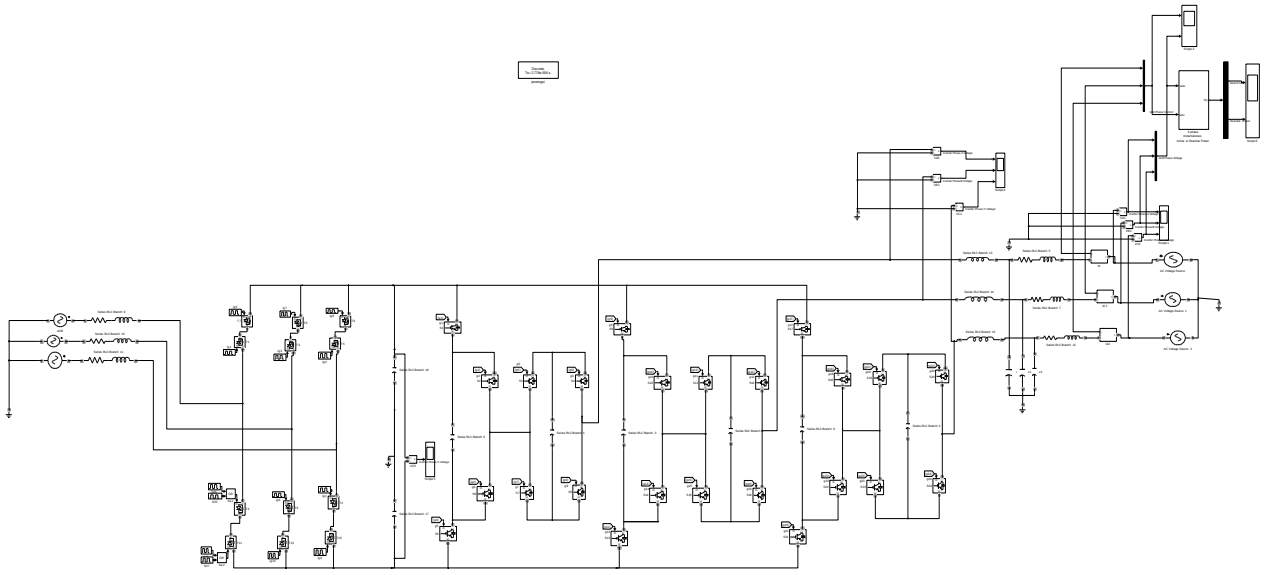

Figure 17: Simulink model of a Back to Back converter.